

## Level compressibility in a critical random matrix ensemble: the second virial coefficient

This article has been downloaded from IOPscience. Please scroll down to see the full text article.

2006 J. Phys. A: Math. Gen. 39 2021

(<http://iopscience.iop.org/0305-4470/39/9/003>)

View [the table of contents for this issue](#), or go to the [journal homepage](#) for more

Download details:

IP Address: 171.66.16.108

The article was downloaded on 03/06/2010 at 05:01

Please note that [terms and conditions apply](#).

# Level compressibility in a critical random matrix ensemble: the second virial coefficient

Vladimir E Kravtsov<sup>1,2</sup>, Oleg Yevtushenko<sup>1</sup> and Emilio Cuevas<sup>3</sup>

<sup>1</sup> The Abdus Salam ICTP, Strada Costiera 11, 34100 Trieste, Italy

<sup>2</sup> Landau Institute for Theoretical Physics, 2 Kosygina st, 117940 Moscow, Russia

<sup>3</sup> Departamento de Física, Universidad de Murcia, E-30071 Murcia, Spain

E-mail: [kravtsov@ictp.trieste.it](mailto:kravtsov@ictp.trieste.it), [bom@ictp.trieste.it](mailto:bom@ictp.trieste.it) and [ecr@um.es](mailto:ecr@um.es)

Received 17 October 2005

Published 15 February 2006

Online at [stacks.iop.org/JPhysA/39/2021](http://stacks.iop.org/JPhysA/39/2021)

## Abstract

We study spectral statistics of a Gaussian unitary critical ensemble of almost diagonal Hermitian random matrices with off-diagonal entries  $\langle |H_{ij}|^2 \rangle \sim b^2 |i - j|^{-2}$  small compared to diagonal ones  $\langle |H_{ii}|^2 \rangle \sim 1$ . Using the recently suggested method of *virial expansion* in the number of interacting energy levels (Yevtushenko and Kravtsov 2003 *J. Phys. A: Math. Gen.* **36** 8265), we calculate a coefficient  $\propto b^2 \ll 1$  in the level compressibility  $\chi(b)$ . We demonstrate that only the leading terms in  $\chi(b)$  coincide for this model and for an exactly solvable model suggested by Moshe *et al* (1994 *Phys. Rev. Lett.* **73** 1497), the sub-leading terms  $\sim b^2$  being different. Numerical data confirm our analytical calculation.

PACS numbers: 02.10.Yn, 71.23.-k, 71.23.An

## 1. Introduction

### 1.1. Critical power-law banded random matrices and exactly solvable models

Recently, there has been an increasing interest to unconventional random matrix theories (RMTs) that interpolate between the Wigner–Dyson RMT and banded RM with the (almost) Poissonian level statistics. One of these models is the *power-law banded random matrix* theory [1–3] for which the variance of the off-diagonal elements takes the form

$$\text{PLBRM: } \langle |V_{ij}|^2 \rangle = \frac{1}{2} \frac{1}{1 + \left(\frac{N}{\pi b} \sin\left(\frac{\pi}{N}|i - j|\right)\right)^{2\alpha}}. \quad (1)$$

Here  $N$  is the matrix size;  $\alpha$  and  $b$  are two parameters which control statistical properties of PLBRM. The variance (1) is nearly constant inside the band  $|i - j| < b$ , and decreases as a power-law function  $\langle |V_{ij}|^2 \rangle \sim 1/|i - j|^{-2\alpha}$  for  $|i - j| > b$ . The case  $\alpha > 1$  corresponds

to the power-law localization which can be found in certain periodically driven quantum-mechanical systems [4]. If  $\alpha \leq 1/2$  the spectral statistics of PLBRM approaches that of the Wigner–Dyson RMT. The special case  $\alpha = 1$  is relevant for the description of critical systems with multifractal eigenstates [1–3, 5, 6], in particular for systems at the Anderson localization–delocalization transition point. On the other hand, it has been conjectured [7] that the spectral statistics of critical PLBRM with large  $b$  can be mapped onto the Calogero–Sutherland model (CS) [8] at low temperature  $T \sim 1/b$ . According to this mapping instead of the spectral problem of random matrices one studies the statistics of one-dimensional fermions in a parabolic confinement potential interacting with the inverse square potential  $(x_i - x_j)^{-2}$  (for real off-diagonal elements in PLBRM, or *the orthogonal ensemble*) or non-interacting (for complex off-diagonal elements in PLBRM with identical distribution of real and imaginary parts, or *the unitary ensemble*).

However, there is a RMT for which the mapping onto the CS model is *exact* [9]. This is the model of Moshe, Neuberger and Shapiro (MNS) [10]. The probability distribution of the Hamiltonian  $\hat{\mathcal{H}}$  in MNS is given by  $P(\hat{\mathcal{H}}) = \int d\hat{U} \mathcal{P}_{\hat{U}}(\hat{\mathcal{H}})$ , where

$$\mathcal{P}_{\hat{U}}(\hat{\mathcal{H}}) \propto \exp \left( -\text{Tr} \hat{\mathcal{H}}^2 - \left( \frac{N}{2\pi b} \right)^2 \text{Tr}([\hat{U}, \hat{\mathcal{H}}][\hat{U}, \hat{\mathcal{H}}^\dagger]) \right); \quad (2)$$

the matrix  $\hat{U}$  is either unitary (for  $\mathcal{H}$  from the unitary ensemble) or orthogonal (for  $\mathcal{H}$  from the orthogonal ensemble), and  $d\hat{U}$  is the Haar measure.

The connection between PLBRM and MNS is especially clear in the unitary case [3], where the unitary matrix  $\hat{U} = M \text{diag}\{e^{i\varphi_i}\} M^\dagger$  can be diagonalized by a unitary transformation. Then the variances of  $V_{i,j} = (M^\dagger \hat{\mathcal{H}} M)_{i,j}$  in MNS at given phases  $\varphi_i$  are

$$\text{MNS} : \quad \langle |V_{ij}|^2 \rangle = \frac{1}{2} \frac{1}{1 + \left( \frac{N}{\pi b} \right)^2 \sin^2 \left( \frac{\varphi_i - \varphi_j}{2} \right)}. \quad (3)$$

One can easily see that equation (3) coincides with equation (1) at  $\alpha = 1$  if the phases  $\varphi_n = 2\pi n/N$  are arranged as an ordered array on a circle. In general, the MNS model can be considered as an extension of the PLBRM model for the case of a random arrangement of phases  $\varphi_n$  distributed over the circle with the joint probability distribution  $P(\{\varphi\})$  [10]:

$$P(\{\varphi\}) \sim \prod_{i>j} \frac{\sin^2 \left( \frac{\varphi_i - \varphi_j}{2} \right)}{1 + \left( \frac{N}{\pi b} \right)^2 \sin^2 \left( \frac{\varphi_i - \varphi_j}{2} \right)}. \quad (4)$$

The averaged value of an observable  $A(\hat{H})$ , which is invariant under the transformation  $\hat{H} \rightarrow M^\dagger \hat{\mathcal{H}} M$ , can be calculated as

$$\langle\langle A \rangle\rangle_{\hat{H}} \equiv \frac{\int \langle A \rangle_{\hat{H}} P(\{\varphi_i\}) \mathcal{D}\{\varphi_i\}}{\int P(\{\varphi_i\}) \mathcal{D}\{\varphi_i\}}. \quad (5)$$

Here  $\langle A \rangle_{\hat{H}}$  stands for the averaging over the Gaussian random matrix  $\hat{H}$  with entries having zero mean value and the variance given by equation (3).

The two-point correlation function, which follows from equation (4) after the integration over all but two phases, was calculated by Gaudin with the help of the model of free non-interacting fermions with a linear spectrum [11]:

$$\mathcal{R}_2(s) = 1 - \frac{1}{(2\pi b)^2} \left| \int_{-\log(e^{2\pi b} - 1)}^{\infty} \frac{e^{i\frac{\omega s}{b}} d\omega}{e^\omega + 1} \right|^2, \quad s \equiv (\varphi_i - \varphi_j)(N/2\pi). \quad (6)$$

If  $|s| \gg b$ , the correlation function is almost constant  $\mathcal{R}_2(|s| \gg b) \rightarrow 1$ . There is a repulsion between phases at a small scale controlled by  $b$ :  $\mathcal{R}_2(|s| \ll b) \sim (s/b)^2$ .

### 1.2. Spectral statistics of MNS and PLBRM

The level statistics of RMT is characterized by the density of states

$$\rho(E) = \left\langle \sum_{n=1}^N \delta(E - \epsilon_n) \right\rangle, \quad (7)$$

and its multi-point correlation functions. For example, the two-level correlation function  $R(\omega)$  is defined as

$$R(\omega) = \frac{\langle\langle \rho(\omega/2)\rho(-\omega/2) \rangle\rangle}{\langle\rho(0)\rangle^2}, \quad \langle\langle \hat{a}\hat{b} \rangle\rangle \equiv \langle \hat{a}\hat{b} \rangle - \langle \hat{a} \rangle \langle \hat{b} \rangle. \quad (8)$$

The Fourier transform of  $R(\omega)$  is known as the spectral form factor  $K(t)$ :

$$K(t) = \int_{-\infty}^{+\infty} e^{i\omega t} R(\omega) d\omega. \quad (9)$$

We rescale time by the mean level spacing

$$\Delta \equiv \frac{1}{\langle\rho(0)\rangle} \quad (10)$$

introducing the dimensionless time  $\tau = t\Delta$ . In the limit of small time the spectral form factor  $K(\tau \rightarrow 0)$  is linked to the other important spectral characteristics called *the level compressibility* [12]:

$$\chi = \lim_{\tau \rightarrow 0} (\lim_{N \rightarrow \infty} K(\tau)). \quad (11)$$

The meaning of  $\chi$  is the following: let us take a window of the width  $\delta E$ ,  $\delta E/\Delta \equiv \bar{n} \ll N$ , in the energy space centred at  $E = 0$  and calculate the number  $n$  of levels inside the window at some realization of disorder. The level number variance is  $\Sigma_2(\bar{n}) = \langle (n - \bar{n})^2 \rangle$ . The level compressibility is by definition the limit

$$\chi = \lim_{\bar{n} \rightarrow \infty} \left( \lim_{N \rightarrow \infty} \frac{\partial \Sigma_2(\bar{n})}{\partial \bar{n}} \right). \quad (12)$$

The level compressibility contains information about the localization transition:  $\chi$  ranges from  $\chi_{\text{WD}} = 0$  for the Wigner–Dyson statistics with extended wavefunctions and a strong levels repulsion to  $\chi_{\text{P}} = 1$  in the case of localized wavefunctions and uncorrelated levels with a Poissonian distribution. The intermediate situation

$$0 < \chi_{\text{crit}} < 1$$

is inherent for the critical regime of multifractal wavefunctions [12].

The exact expression for the level compressibility in the unitary MNS reads [13]

$$\chi_{\text{MNS}} = \frac{\text{Li}_{-\frac{1}{2}}[1 - \exp(2\pi b)]}{\text{Li}_{+\frac{1}{2}}[1 - \exp(2\pi b)]} \simeq \begin{cases} 1/(4\pi b), & b \gg 1, \\ 1 - \sqrt{2\pi} b, & b \ll 1, \end{cases} \quad (13)$$

where  $\text{Li}$  is the polylogarithm function [14]. One can see that  $\chi_{\text{MNS}}$  obeys an inequality  $0 < \chi_{\text{MNS}} < 1$ , at any finite  $b$ .

Moreover, the level statistics of MNS and of critical PLBRM are asymptotically the same in two limits:  $b \rightarrow 0$  and  $b \rightarrow \infty$ .

If  $b \gg 1$ , the theory of critical PLBRM with  $\alpha = 1$  can be rigorously developed by mapping [1] onto the nonlinear supersymmetric  $\sigma$ -model [15]. One can show that the level statistics of critical PLBRM approaches the Wigner–Dyson statistics [2, 3, 7]. In particular,

the level compressibility of PLBRM goes to zero and asymptotically coincides with the compressibility for MNS:

$$b \gg 1 \Rightarrow \chi_{\text{PLBRM}}|_{\alpha=1} \simeq \chi_{\text{MNS}} \simeq \frac{1}{4\pi b} + O(b^{-2}) \ll 1. \quad (14)$$

This is because the phase repulsion in MNS is strong at large  $b$ . The phases  $\varphi_{i,j}$  form an approximately equidistant lattice-like structure [3].

In the opposite case  $b \ll 1$ , the phase repulsion in MNS is weak and the phases  $\varphi_{i,j}$  do not form a regular structure. The disorder in the phase arrangements at a small distance  $|\varphi_i - \varphi_j| \leq 1/N$  may become especially important and, therefore, there is no *a priori* evident correspondence between critical PLBRM and MNS at  $b \ll 1$ .

Let us consider the  $N \rightarrow \infty$  limit of equation (1) at  $\alpha = 1$ . If  $b \ll 1$  the off-diagonal matrix elements of such a PLBRM are parametrically small compared to the diagonal ones:

$$\alpha = 1, b \ll 1: \quad \langle \varepsilon_i^2 \rangle = \frac{1}{\beta} \gg \langle |V_{ij}|^2 \rangle \simeq b^2 \mathcal{F}(i-j), \quad \mathcal{F}(i-j) = \frac{1}{2} \frac{1}{(i-j)^2}. \quad (15)$$

We will refer to equation (15) as the *almost diagonal critical PLBRMs*. The parameter  $\beta$  corresponds to the Dyson symmetry classes:  $\beta_{\text{GOE}} = 1$  for the Gaussian orthogonal ensemble, and  $\beta_{\text{GUE}} = 2$  for the Gaussian unitary ensemble.

This model cannot be mapped onto the nonlinear sigma model as the mapping is only justified if  $b \gg 1$ . At  $b \ll 1$ , the compressibility of PLBRM and MNS is close to the Poissonian value  $\chi_P = 1$ . The leading correction of the order of  $O(b)$  was derived in [2, 16] using an approximation of two interacting levels first suggested in [6]. Surprisingly, disorder in the arrangement of MNS phases does not influence  $\chi$  and the compressibilities for PLBRM and MNS are again asymptotically the same:

$$b \ll 1 \Rightarrow \chi_P - \chi_{\text{PLBRM}}|_{\alpha=1} \simeq \chi_P - \chi_{\text{MNS}} \simeq \sqrt{2\pi} b + O(b^2) \ll 1. \quad (16)$$

### 1.3. Formulation of the problem

A natural question arises as to whether the level rigidities of critical PLBRM and MNS coincide at an arbitrary  $b \sim 1$ . The numerical simulations [13] did not exclude such a possibility. The main result of this paper is that it is not the case: the sub-leading corrections of order  $O(b^2)$  are different in those two models. To prove this statement we analytically calculate *the second coefficient of the virial expansion* [16] for the level compressibility for the critical PLBRM of the unitary symmetry class and compare it with the exact result (13) for MNS.

As the analytical calculation is quite involved we undertook an extensive numerical investigation of the same problem and found an excellent agreement with the analytical prediction.

This paper is organized as follows: we briefly discuss the virial expansion in section 2 and re-derive equation (16) as the first virial coefficient in section 3. The main result of the present paper, namely, *the second virial coefficient* for unitary critical PLBRM, is calculated in section 4. The analytical result is confirmed by the direct numerical simulations which are presented in section 4.3. We end the paper with a brief discussion and conclusions.

## 2. The virial expansion

The virial expansion (VE) is a method that allows us to study spectral statistics of a disordered system described by a Gaussian ensemble of the Hermitian  $N \times N$  ( $N \gg 1$ ) almost diagonal random matrices which have random independent elements [16, 17]:

$$\langle H_{i,j} \rangle = 0, \quad \langle H_{i,i}^2 \rangle \gg \langle |H_{i \neq j}|^2 \rangle.$$

It is an *expansion in the number of interacting energy levels*. Unlike the field-theoretical approach, VE starts from the Poissonian statistics and yields a *regular expansion* in powers of the small parameter controlling the ratio of the off-diagonal elements to the diagonal ones  $\langle |H_{i \neq j}|^2 \rangle / \langle H_{ii}^2 \rangle \sim b^2 \ll 1$ . The expansion has been represented by the summation of diagrams which are generated with the help of the Trotter formula. A rigorous selection rule has been established for the diagrams, which allows us to account for exact contributions of a given number of resonant and non-resonant interacting levels. The method offers a controllable way to find an answer to the question when a weak interaction of levels can drive the system from localization towards criticality and delocalization. An example of the spectral form factor has been considered in [16] for a generic dependence of the variance  $\langle |H_{i \neq j}|^2 \rangle$  on the difference  $i - j$ . It has been shown that a term of the order of  $b^{c-1}$  is governed by the interaction of  $c$  energy levels. VE has been applied to DOS in [17].

VE has been described in detail in [16]. Here, we repeat only its basic definitions and final results which will be applied to the model (15). VE deals with the following correlation function in the time domain:

$$\tilde{K}(N, \tau) = \frac{1}{N} \langle \text{Tr} e^{-i\hat{H}\tau/\Delta} \text{Tr} e^{i\hat{H}\tau/\Delta} \rangle \equiv \tilde{K}_0(N, \tau) + b\tilde{K}_1(N, \tau) + b^2\tilde{K}_2(N, \tau) + \dots \quad (17)$$

For the constant mean density of states  $\tilde{K}$  coincides with  $K$ . However, they are different if  $\langle \rho(E) \rangle$  essentially depends on energy  $E$ . In analogy with equation (11) one can define the quantity

$$\chi_0 \equiv \lim_{\tau \rightarrow 0} \left( \lim_{N \rightarrow \infty} \tilde{K}(N, \tau) \right). \quad (18)$$

It turns out that at small  $b$  there is a simple approximate relationship between  $\chi$  and  $\chi_0$  (see the appendix of the paper [16]):

$$\chi \simeq 1 - \frac{1 - \chi_0}{\Upsilon}, \quad \Upsilon = \frac{\Delta}{N} \int_{-\infty}^{+\infty} \langle \rho(E) \rangle^2 dE. \quad (19)$$

The mean density of states for the Gaussian ensemble of almost diagonal RMs with either localized or (sparse) fractal eigenstates is close to the Gaussian distribution of the diagonal entries [17]:

$$\langle \rho(E) \rangle \simeq N \sqrt{\frac{\beta}{2\pi}} \exp\left(-\frac{\beta E^2}{2}\right) \Rightarrow \Delta \simeq \frac{1}{N} \sqrt{\frac{2\pi}{\beta}}. \quad (20)$$

The corrections to this formula start with terms proportional to  $b^2$ . Thus with an accuracy of  $O(b^2)$  the unfolding factor in equation (19) can be taken as  $\Upsilon^{-1} \simeq \sqrt{2}$ .

Each function  $\tilde{K}_i$  is governed by the interaction of the  $i + 1$  energy levels. The perturbative expansion (17) is valid if the limit  $\lim_{N \rightarrow \infty} (\tilde{K}_i)$  is finite. This can be secured by a separation of scales: the level interaction is effectively large at the distances  $|\omega| < \Omega_{\text{int}} = b\Delta$  which are parametrically smaller than the mean level spacing  $\Delta$ . Otherwise, VE fails and one has to take into account an infinite number of interacting levels.

### 3. Leading correction to Poissonian level compressibility

Expansion (17) starts with the Poissonian form factor  $K_P$

$$\lim_{N \rightarrow \infty} \tilde{K}_0 = K_P = 1$$

reflecting a distribution of uncorrelated diagonal matrix elements. The functions  $\tilde{K}_i$  are given by power series in a large parameter

$$x = \tilde{N}|\tau|b, \quad \tilde{N} \equiv \Delta^{-1} \propto N. \quad (21)$$

The first correction  $b\tilde{K}_1$  to the Poissonian spectral statistics is governed by the interaction of two energy levels. The series for the function  $\tilde{K}_1$  in GOE and GUE reads

$$\tilde{K}_1 = 2\sqrt{\pi\beta} \sum_{k=1}^{\infty} (-1)^k C_{\beta}^{(2)}(k) \mathcal{R}_N^{(1)}(k) x^{2k-1}, \quad (22)$$

$$C_{\beta=1}^{(2)}(k) = \frac{(2k-1)!!}{k!(k-1)!}, \quad (23)$$

$$C_{\beta=2}^{(2)}(k) = \frac{1}{(k-1)!}. \quad (24)$$

In equation (22), we introduce the real-space sum which depends on the correlation function  $\mathcal{F}$  defined in equation (15):

$$\mathcal{R}_N^{(1)}(k) \equiv \frac{1}{2} \sum'_m (\mathcal{F}(m))^k = \frac{\zeta(2k)}{2^{2k}} + O(1/N), \quad \sum'_m = \sum_{m=-N}^{-1} + \sum_{m=1}^N, \quad (25)$$

where  $\zeta$  is the Riemann zeta function [14]. The  $1/N$ -corrections in (25) yield the dependence of  $\tilde{K}_1$  on a parameter  $|\tau|b = x/N$ .

To derive the compressibility  $\chi_0$ ,

$$\chi_0 \simeq 1 + b\chi_0^{(1)},$$

we have to put  $\tau = 0$  after doing the limit  $x \rightarrow \infty$ :

$$\chi_0^{(1)} = \lim_{\tau \rightarrow 0} (\lim_{x \rightarrow \infty} (\tilde{K}_1(x, \tau b))). \quad (26)$$

The small time limit means that we have to neglect all the  $1/N$ -corrections in equation (25). It is achieved if one substitutes  $\mathcal{R}^{(1)}(k) = \lim_{N \rightarrow \infty} \mathcal{R}_N^{(1)}(k)$  for  $\mathcal{R}_N^{(1)}(k)$ :

$$\mathcal{R}^{(1)}(k) = \sum_{m=1}^{\infty} (\mathcal{F}(m))^k. \quad (27)$$

It is convenient to insert equation (27) into the series (22) and to sum over  $k$  prior to the summation over  $m$ :

$$\tilde{K}_1(\tau = 0) \simeq -\sqrt{\beta\pi} \sum_{m=1}^{\infty} \frac{x}{m^2} \exp\left(-\frac{x^2}{2m^2}\right) \begin{cases} I_0\left(\frac{x^2}{2m^2}\right) - I_1\left(\frac{x^2}{2m^2}\right), & \beta = 1, \\ 1, & \beta = 2. \end{cases} \quad (28)$$

Here  $I_{0,1}(\dots)$  are the modified Bessel functions [14]. The sum over  $m$  converges at  $m \sim x \gg 1$ ; therefore, it can be converted to the integral  $\int_0^{\infty} dm$ . After this integration we find

$$\chi_0^{(1)}|_{\beta=1} = -2, \quad \chi_0^{(1)}|_{\beta=2} = -\pi. \quad (29)$$

#### 4. Correction to level compressibility of order $b^2$

##### 4.1. The second virial coefficient for the critical PLBRM

Now we focus on the term of the order  $O(b^2)$  in equation (17), which is governed by the interaction of the three energy levels. In the unitary case, we will be considering below the expression for  $\tilde{K}_2$  as [16]

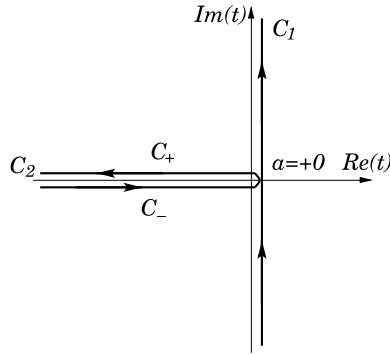


**Figure 1.** The integration contours for the variable  $t$ :  $C_1 : \{\text{Re}(t) = a > 0, \text{Im}(t) \in ]-\infty; +\infty[ \}$  and  $C_2 = C_+ \cup C_-$ , where  $C_- = \{\text{Re}(t) \in ]-\infty; a], \text{Im}(t) = -0\}$ ;  $C_+ = \{\text{Re}(t) \in [a; -\infty[, \text{Im}(t) = +0\}$ . One can put  $a = +0$ .

$$\beta = 2 : \quad \tilde{K}_2 = \frac{2}{\sqrt{3}} \sum_{k_1, k_2, k_3=0}^{\infty} (-1)^{k_1+k_2+k_3} C^{(3)}(k_1, k_2, k_3) \mathcal{R}_N(k_1, k_2, k_3) x^{2(k_1+k_2+k_3)-2} \quad (30)$$

$$C^{(3)} = \frac{2k_1k_2k_3 - k_1k_2 - k_2k_3 - k_1k_3}{\Gamma(k_1 + k_2 + k_3 - 3/2)} \frac{\Gamma(k_1 - 1/2)}{\Gamma(k_1 + 1)} \frac{\Gamma(k_2 - 1/2)}{\Gamma(k_2 + 1)} \frac{\Gamma(k_3 - 1/2)}{\Gamma(k_3 + 1)}, \quad (31)$$

$$\mathcal{R}_N(\{k_i\}) = \frac{1}{6} \sum'_{m,n} \Big|_{m \neq n} [(\mathcal{F}(m))^{k_1} (\mathcal{F}(n))^{k_2} (\mathcal{F}(|m-n|))^{k_3}]. \quad (32)$$

The series on the rhs of equation (30) is three-dimensional. It cannot be reduced to a product of one-dimensional series because of the function  $\Gamma^{-1}(k_1 + k_2 + k_3 - 3/2)$  in the coefficient (31). We will decouple the sums over the indices  $k_{1,2,3}$  using an integral representation [18] of the function  $\Gamma^{-1}(z)$  :

$$\frac{1}{\Gamma(z)} = \frac{1}{2\pi i} \int_{C_1} \frac{\exp(t)}{t^z} dt; \quad (33)$$

the integration contour  $C_1$  is shown in figure 1. Then, we change the order of summations over  $k_i$  and integration over  $t$ . The real-space summation which is implied in the function  $\mathcal{R}_N$  has to be done at the last step. We assume further that the sums over  $m$  and  $n$  converge at large values of the summation variables and transform the sums into a two-fold integral (in analogy with the derivation of  $\chi_0^{(1)}$ ). This assumption is verified below (see section 4.2). Using the identities

$$\sum_{k=0}^{\infty} (-y)^k \frac{\Gamma(k - 1/2)}{\Gamma(k + 1)} = -2\sqrt{\pi} \sqrt{1+y},$$

$$\sum_{k=1}^{\infty} (-y)^k k \frac{\Gamma(k - 1/2)}{\Gamma(k + 1)} = -\sqrt{\pi} \frac{y}{\sqrt{1+y}}$$

and substituting  $\infty$  for  $N$  in the limits of the real-space integrals over  $m$  and  $n$  (in analogy with equation (27)) we arrive at the following expression:

$$\tilde{K}_2(x, \tau = 0) = \frac{\iota x}{6} \sqrt{\frac{\pi}{3}} \int \int_{-\infty}^{+\infty} dm dn \int_{C_1} dt \exp(t) \bar{P}_{|n|} \bar{P}_{|m|} (\bar{P}_{|m-n|} - 3\bar{Q}_{|m-n|}), \quad (34)$$

where

$$P(y) = \frac{y}{\sqrt{1+y}}, \quad \bar{P}_{|j|} \equiv \frac{\sqrt{t}}{x} P\left(\frac{x^2}{j^2 t}\right), \quad (35)$$



$$Q(y) = \sqrt{1+y}, \quad \bar{Q}_{|j|} \equiv \frac{\sqrt{t}}{x} Q\left(\frac{x^2}{j^2 t}\right), \quad (36)$$

and we have absorbed  $1/\sqrt{2}$  into  $x$  obtaining  $1/2$  as a common prefactor. The integrand in equation (34) as the function of  $t$  has a branching point  $t = 0$ . A branch cut may be drawn along the negative semi-axis. Since the integrand in equation (34) is zero if  $|t| \rightarrow \infty$  at  $\text{Re}(t) \leq a = +0$  and has poles neither in upper nor in lower half-planes, we can transform the integration contour  $C_1$  into  $C_2 = C_+ \cup C_-$  (see figure 1) which encloses the branch cut. Fourier transforming the functions (35) and (36) and using a scaled spatial coordinate

$$J = j/x,$$

we find the  $x$ -independent expression for  $\tilde{K}_2$ :

$$\tilde{K}_2(\tau = 0) = \frac{4t}{3\sqrt{3}\pi} \lim_{\eta \rightarrow +0} \left\{ \int_0^{+\infty} d\mathcal{M} \int_{C_2} dt \exp(t) F_1^2(F_1 - 3F_2) \right\}, \quad (37)$$

$$F_1(\mathcal{M}, t) = \int_{\eta}^{+\infty} dJ \frac{\cos(J\mathcal{M})}{J\sqrt{1+J^2t}}, \quad (38)$$

$$F_2(\mathcal{M}, t) = \int_{\eta}^{+\infty} dJ \frac{\cos(J\mathcal{M})}{J} \sqrt{1+J^2t}. \quad (39)$$

We have introduced an infinitesimal positive constant  $\eta$ , which regularizes the integrals (38) and (39) at small distances. We will show that  $\tilde{K}_2(\tau = 0)$  is finite at  $\eta \rightarrow +0$  thus proving that the small distances do not play a role.

Let us separate out real and imaginary parts of  $F_{1,2}(\mathcal{M}, t \in C_2)$  accounting for a branch cut of  $F_{1,2}$  as functions of  $t$  along the negative semi-axis:

$$F_{1,2}|_{t \in C_2} = F_{1,2}^{(-)}(M) + \iota \text{sign}(\text{Im}(t)) F_{1,2}^{(+)}(M), \quad M \equiv \frac{\mathcal{M}}{\sqrt{|t|}},$$

$$\text{sign}(\text{Im}(t)) = \begin{cases} 1, & \text{if } t \in C_+, \\ -1, & \text{if } t \in C_-; \end{cases}$$

$$F_1^{(+)} = \int_1^{+\infty} dJ' \frac{\cos(MJ')}{J' \sqrt{1-(J')^2}} = -\frac{\pi}{2} \int_M^{\infty} dy J_0(y), \quad (40)$$

$$F_2^{(+)} = \int_1^{+\infty} dJ' \frac{\cos(MJ')}{m} \sqrt{1-(J')^2} = F_1^{(+)}(M) + \frac{\pi}{2} (2\delta(M) - J_1(M)); \quad (41)$$

$$F_1^{(-)} = \int_{\eta}^1 dJ' \frac{\cos(MJ')}{J' \sqrt{1-(J')^2}} = -\frac{\pi}{2} \int_0^M dy H_0(y) + [\text{Ci}(M) - \text{Ci}(\eta M)], \quad (42)$$

$$F_2^{(-)} = \int_{\eta}^1 dJ' \frac{\cos(MJ')}{J'} \sqrt{1-(J')^2} = F_1^{(+)}(M) - \frac{\pi}{2} H_{-1}(M). \quad (43)$$

Here,  $J_{0,1}$  are the Bessel functions,  $H_{0,-1}$  are the Struve functions and Ci is the cosine integral function [14]. We will use the property

$$\lim_{\eta \rightarrow +0} [\text{Ci}(M) - \text{Ci}(\eta M) + \log(\eta)] = 0.$$

One can see that the integral of the real part of  $F_1^2(F_1 - 3F_2)$  over  $t$  is zero due to a cancellation of the integrals over  $C_+$  and  $C_-$ . Thus, we may keep only the imaginary part of  $F_1^2(F_1 - 3F_2)$  in equation (37):

$$F_1^2(F_1 - 3F_2) \rightarrow \iota \operatorname{sign}(\operatorname{Im}(t))[\Theta_1(M) + \Theta_2(M)], \tag{44}$$

$$\Theta_1(M) \equiv 3(F_1^{(+)} )^2 F_2^{(+)} - (F_1^{(+)} )^3, \tag{45}$$

$$\Theta_2(M) \equiv 3(F_1^{(-)} )^2 (F_1^{(+)} - F_2^{(+)} ) - 6F_1^{(-)} F_2^{(-)} F_1^{(+)} . \tag{46}$$

We insert equation (44) into expression (37):

$$\iota \int_0^{+\infty} dM F_1^2(F_1 - 3F_2) \int_{C_2} dt \exp(t) \rightarrow 2 \int_0^{+\infty} dM (\Theta_1 + \Theta_2) \int_0^\infty dt \sqrt{t} \exp(-t), \tag{47}$$

and integrate over  $t$  obtaining

$$\chi_0^{(2)} = \frac{4}{3\sqrt{3}} \lim_{\eta \rightarrow +0} \left\{ \int_0^{+\infty} dM (\Theta_1(M) + \Theta_2(M)) \right\}. \tag{48}$$

Let us consider the first integral on the rhs of equation (48):

$$\begin{aligned} \mathcal{I}_1 &\equiv \int_0^{+\infty} dM \Theta_1(M) \\ &= \left(\frac{\pi}{2}\right)^3 \int_0^{+\infty} dM \left\{ 3 \left( \int_M^\infty dy J_0(y) \right)^2 (2\delta(M) - J_1(M)) - 2 \left( \int_M^\infty dy J_0(y) \right)^3 \right\}. \end{aligned} \tag{49}$$

We note that the integrals in equation (49) does not contain the regularizer  $\eta$ . The first term with the  $\delta$ -function can be immediately integrated using  $\int_0^\infty dy J_0(y) = 1$  [18]. The other two terms can be integrated by parts with the help of the standard integrals containing the Bessel functions [18]. The result reads

$$\mathcal{I}_1 = \frac{3\pi^3}{4} \int_0^\infty dM (M [J_0(M)]^3) = \frac{\sqrt{3}\pi^2}{2}. \tag{50}$$

Finally, we have to calculate the second integral on the rhs of equation (48):

$$\begin{aligned} \mathcal{I}_2 &\equiv \int_0^{+\infty} dM \Theta_2(M) = 6 \left(\frac{\pi}{2}\right)^3 \lim_{\Omega \rightarrow +\infty} \left[ \int_0^\Omega dM \left\{ \left( \int_0^M dy H_0(y) - \log(\eta) \right)^2 \right. \right. \\ &\quad \times \left( \frac{J_1(M)}{2} - \delta(M) + \int_M^\infty dy J_0(y) \right) + H_{-1}(M) \\ &\quad \left. \left. + \left( \int_0^M dy H_0(y) - \log(\eta) \right) \int_M^\infty dy J_0(y) \right\} \right]. \end{aligned} \tag{51}$$

Unlike the integral  $\mathcal{I}_1$ , the regularizer of the small distances  $\eta$  enters the expression for the integral  $\mathcal{I}_2$ . We have also introduced the upper limit of the integration over  $M$  before integrating equation (51) by parts. At intermediate stages, the boundary terms of the integration by parts, which result from the different parts of the integrand on the rhs of (51), diverge in the limits  $\eta \rightarrow 0$  and  $\Omega \rightarrow \infty$ . However, the diverging contributions *exactly cancel out* at the end so that the final answer for  $\mathcal{I}_2$  does not depend on  $\eta$  and is finite in the limit  $\Omega \rightarrow \infty$ . For example, the coefficient in front of  $\log^2(\eta)$

$$\lim_{\Omega \rightarrow +\infty} \left\{ \int_0^\Omega dM \left( \frac{J_1(M)}{2} - \delta(M) + \int_M^\infty dy J_0(y) \right) \right\}$$

is zero because

$$\int_0^\infty dy J_1(y) = 2 \int_0^\infty dy \delta(y) = 1,$$

$$\lim_{\Omega \rightarrow +\infty} \left\{ \int_0^\Omega dM \int_M^\infty dy J_0(y) \right\} = - \lim_{\Omega \rightarrow +\infty} \left\{ \Omega \left( \int_\Omega^\infty dy \frac{J_1(y)}{y} \right) \right\} \propto \lim_{\Omega \rightarrow +\infty} \frac{1}{\sqrt{\Omega}} = 0.$$

The cancellation of  $\log(\eta)$  can be checked in a similar way. We have thus proven that the regularization of the Fourier images (38) and (39) does not affect the level compressibility.

We skip a lengthy intermediate integration by parts and present only the answer for  $\mathcal{I}_2$ :

$$\mathcal{I}_2 = 3\pi^2 \int_0^\infty dM (H_0(M) J_0(M)) - \frac{9\pi^3}{4} \int_0^\infty dM (M H_0(M)^2 J_0(M)). \quad (52)$$

To our best knowledge, the integrals of a combination of the Bessel function and the Struve function on the rhs of equation (52) are not included in the standard handbooks. We describe their calculation in appendices. Here, we give the results

$$\int_0^\infty dM (H_0(M) J_0(M)) = \frac{1}{2}, \quad (53)$$

$$\int_0^\infty dM (M H_0(M)^2 J_0(M)) = \frac{2}{\pi} \left( 1 - \frac{1}{\sqrt{3}} \right), \quad (54)$$

$$\Rightarrow \mathcal{I}_2 = \frac{3\pi^2}{2} (\sqrt{3} - 2t), \quad \mathcal{I}_1 + \mathcal{I}_2 = (2 - \sqrt{3})\sqrt{3}\pi^2, \quad \chi_0^{(2)} = (2 - \sqrt{3}) \frac{4\pi^2}{3}. \quad (55)$$

We insert formulae (29) and (55) into equation (19) and obtain the expression for the level compressibility of the critical unitary PLBRMs:

$$\beta = 2: \quad \chi = 1 - \sqrt{2} \left[ (\pi b) - \frac{4}{3} (2 - \sqrt{3})(\pi b)^2 \right] + O(b^3). \quad (56)$$

#### 4.2. Characteristic spatial scale that governs the compressibility

Let us estimate the characteristic spatial scale that governs the second virial coefficient  $\chi_0^{(2)}$ . Firstly, we note that all integrals over  $t$  and  $M$  converge at  $|t|_{\text{char}} \sim 1$  (see equations (47) and (48)) and  $M_{\text{char}} \sim 1$  (see equations (50), (53) and (54)). Returning to the spatial variable  $j = xJ$ , we may estimate its characteristic scale:

$$j_{\text{char}} \sim x J_{\text{char}} \sim x / M_{\text{char}} \sim x \sqrt{|t|_{\text{char}} / M_{\text{char}}} \sim x \gg 1.$$

Therefore,  $\chi_0^{(2)}$  is governed by the large distances  $m, n, (m - n) \sim x \gg 1$  (see equation (34)). We have verified the self-consistency of our calculation scheme for  $\chi_0^{(2)}$ ; namely, the replacement of the real-space sum by the integral is justified.

The first virial coefficient  $\chi_0^{(1)}$  is also governed by the large distances of the order of  $x$  (see equation (28)). We may conclude that the small distances do not contribute to the compressibility. One important consequence is that the level compressibility is not sensitive to the periodicity of the boundary conditions. If we recalculated  $\chi_0^{(1,2)}$  using the spatially periodic variance (1) instead of (15) we would again arrive at the same results (29) and (55).

#### 4.3. Numerical test of the results

A comparison of the analytical result (56) with the direct numerical calculation of  $\chi$  is presented in figure 2. The data correspond to equation (1) with  $b = 0.1$  for the unitary symmetry,  $\beta_{\text{GUE}} = 2$ .

Numerical calculations were done in the range  $200 \leq N \leq 10\,000$ . The true value of  $\chi$  is found from the extrapolation of numerically obtained  $\chi(N)$  to  $N \rightarrow \infty$ .

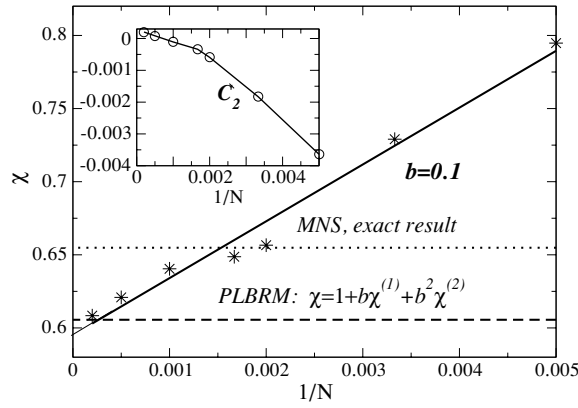


**Figure 2.** A comparison of the analytical result (56) with the direct numerical calculation of  $\chi$  at  $b = 0.1$ : stars mark the result of simulations at the different matrix sizes; the solid line is an interpolation that yields  $\chi|_{N \rightarrow \infty} = 0.595 \pm 0.005$ ; dashed horizontal lines give the analytical result  $\chi \approx 0.605$  (56) for  $b = 0.1$ ; the dotted line presents the compressibility of unitary MNS. Inset: the coefficient  $C_2$  of the polynomial fitting equation (57) for  $\Sigma_2$  as a function of  $1/N$ .

The number of realizations ranges from 30 000 for the small matrix size ( $N = 200$ ) to 200 for the larger one ( $N = 10\,000$ ). The level compressibility has been obtained from the level number variance  $\Sigma_2(\bar{n}) = \langle (n - \bar{n})^2 \rangle$ :  $\Sigma_2(\bar{n})$  has been calculated in a small energy window  $\delta E \approx 0.4$  at the band centre<sup>4</sup>. Then, the  $N$ -dependent spectral compressibility  $\chi(N)$  has been obtained for each value of  $N$  as a coefficient of the linear term of a second-order polynomial fit for  $\Sigma_2(\bar{n})$  [13]:

$$\Sigma_2(\bar{n}, N) = C_0(N) + \chi(N)\bar{n} + C_2(N)\bar{n}^2. \quad (57)$$

The fitting range is  $1 < \bar{n} < 100$ . To increase the accuracy, we have done both disorder and spectral averaging of the data. We have also checked that a small change in the window width or in the fitting range practically does not change the results.

For the critical RMT, it is expected [13] that both  $\chi$  and  $C_2$  have a pronounced ( $\propto 1/N$ )  $N$ -dependence reflecting the finite size effects in  $\Sigma_2(\bar{n}, N)$ . The true value of  $\chi$  is obtained at the intersection of the solid line with the vertical axis at the point

$$\chi|_{N \rightarrow \infty} = 0.595 \pm 0.005 \quad (58)$$

(see figure 2) which should be compared to the analytical results for the critical PLBRM and the MNS exact result given by equations (56) and (13), respectively,

$$\lim_{N \rightarrow \infty} \chi_{\text{PLBRM}}(b = 0.1) = 0.6056, \quad \lim_{N \rightarrow \infty} \chi_{\text{MNS}}(b = 0.1) = 0.6548. \quad (59)$$

Given an expectation that the missing term of order  $b^3 \sim 0.001$  is negative (as well as the term of order  $b$ ) and thus equation (56) *overestimates*  $\chi$  by several parts of  $10^{-3}$ , the numerical result is very close to the analytical one and is clearly different to the MNS exact result.

The true value of  $C_2$  is expected to be zero [13]. Indeed, the numerically obtained coefficient  $C_2$  goes to zero as  $N$  increases (see the inset of figure 2). This behaviour of  $C_2$  confirms the good quality of our numerics.

<sup>4</sup> For the small matrix sizes the window was slightly increased in order to get sufficient averaged number of the energy levels (around 100) inside the window.

## 5. Conclusions and discussion

As we have already mentioned in the introduction, the level compressibility of the unitary critical PLBRM and of MNS are asymptotically the same both at  $b \gg 1$  [2, 3] and at  $b \ll 1$  with the accuracy up to the terms of orders  $1/b$  and  $b$ , respectively. While such a coincidence is natural at  $b \gg 1$ , its origin for  $b \ll 1$  still remains unclear.

The main result of this paper, equation (56), is an analytical calculation of the level compressibility for the critical PLBRM ensemble up to the terms of order  $b^2$  and its comparison with the corresponding formula for the MNS model of the unitary symmetry class.

Our result (56) shows that the compressibility in MNS is larger compared to PLBRM:

$$\beta = 2 : \quad \chi|_{\text{MNS}} - \chi|_{\text{PLBRM}} \simeq \frac{\sqrt{2}}{3} (4\sqrt{3}(1 + \sqrt{2}) - (11 + 3\sqrt{2}))(\pi b)^2$$

in agreement with the numerical simulations for PLBRM (see figure 2). It is also important that result (56) is expressible in a simple algebraic form. The fact that all the intermediate sums and integrals can be done exactly in terms of elementary functions is not trivial and may indicate that the PLBRM theory is exactly solvable.

Thus, we conclude that the level compressibility for PLBRM and MNS is *not identical* though very close to each other [13]. It is tempting to assume that the coincidence is a consequence of a certain relation between  $\chi(b)$  and  $\chi(1/b)$  which holds for both models, so that the asymptotic coincidence in spectral statistics for  $b \gg 1$  automatically leads to that for  $b \ll 1$ . This scenario can also be related to the existence of a field-theoretical description [19] which is *dual* to that of the nonlinear sigma model.

Based on the leading terms in the  $b$  and  $1/b$  expansions one can guess a possible form of a relation between  $\chi(b)$  and  $\chi(1/b)$  which can then be checked using the  $b^2$  and  $1/b^2$  terms. From this viewpoint our result (56) is also a very useful step.

However, maybe the most important conclusion we may draw from the above consideration is that the *virial expansion* method [16] is working and helps to obtain solutions to very non-trivial problems.

## Acknowledgments

EC thanks the FEDER and the Spanish DGI for financial support through project no. FIS2004-03117.

## Appendix. Integrals containing product of Bessel and Struve functions

In this appendix, we compute the integrals

$$\text{Int}_1 = \int_0^\infty H_0(x) J_0(x) dx, \quad \text{Int}_2 = \int_0^\infty x H_0^2(x) J_0(x) dx. \quad (\text{A.1})$$

*Integral Int<sub>1</sub>*. Using the integral representation of the Struve function  $H_0$  we convert  $\text{Int}_1$  to the following form:

$$\text{Int}_1 = \frac{2}{\pi} \lim_{\alpha \rightarrow +0} \int_0^1 \frac{dt}{\sqrt{1-t^2}} \text{Im} \left( \int_0^\infty dx J_0(x) \exp[(-\alpha + it)x] \right).$$

The inner integral over  $x$  is zero [18] at  $0 < t < 1$ ,  $\alpha = 0$  and diverges at  $t = 1$ ,  $\alpha = 0$ .

$$\int_0^\infty dx J_0(x) \sin(tx) = \begin{cases} 0, & \text{if } 0 < t < 1, \\ \infty, & \text{if } t = 1. \end{cases}$$

Thus, we see that  $\text{Int}_1$  is determined by the integration over a small vicinity of the point  $t = 1$ . The infinitesimal parameter  $\alpha$  has been introduced to solve an uncertainty  $\|0 \times \infty\|$  with zero coming from the phase volume at  $t \rightarrow 1$ . We calculate the integral over  $x$  keeping the finite  $\alpha$ :

$$\text{Int}_1 = -\frac{1}{\pi} \lim_{\alpha \rightarrow +0} \int_0^1 \frac{dt'}{\sqrt{t'}} \text{Im} \left\{ \frac{1}{\sqrt{t' - i\alpha}} \right\} \equiv \frac{1}{\pi} \int_0^\infty \frac{dz}{\sqrt{z(z^2 + 1)}} \text{Re} \{ \sqrt{-(z + i)} \}, \quad (\text{A.2})$$

$$t' = 1 - t, \quad z = \frac{t'}{\alpha}.$$

Answer (53) results from (A.2) after the substitution

$$-(z + i) = \sqrt{z^2 + 1} \exp(i[\pi + \arctan(1/z)]).$$

*Integral Int<sub>2</sub>.* Let us introduce two auxiliary three-fold integrals

$$I_2^{(1,2)} = \frac{2}{\pi^2} \int_0^1 \int_0^1 \frac{dx}{\sqrt{1-x^2}} \frac{dy}{\sqrt{1-y^2}} \int_0^\infty dq q J_0(q) \cos(q[x \pm y]) \quad (\text{A.3})$$

noting that

$$I_2^{(1)} + I_2^{(2)} = \int_0^\infty dq q J_0^3(q) = \frac{2}{\sqrt{3}\pi}, \quad \text{Int}_2 = I_2^{(2)} - I_2^{(1)} \equiv 2I_2^{(2)} - \frac{2}{\sqrt{3}\pi}.$$

The idea as how to calculate  $I_2^{(2)}$  is very similar to the calculation of  $I_1$ : we use the property [18]

$$\int_0^\infty dq q J_0(q) \cos(q[x - y]) = \begin{cases} 0, & \text{if } -1 < x - y < 1, \\ \infty, & \text{if } x - y = \pm 1, \end{cases}$$

introduce an infinitesimal regularizing parameter

$$I_2^{(2)} = \frac{2}{\pi^2} \lim_{\alpha \rightarrow +0} \int_0^1 \int_0^1 \frac{dx}{\sqrt{1-x^2}} \frac{dy}{\sqrt{1-y^2}} \text{Re} \left\{ \int_0^\infty dq q J_0(q) \exp(-\alpha q + i q[x - y]) \right\}, \quad (\text{A.4})$$

integrate over  $q$  keeping the finite  $\alpha$ :

$$I_2^{(2)} = \frac{2}{\pi^2} \lim_{\alpha \rightarrow +0} \int_0^1 \int_0^1 \frac{dx}{\sqrt{1-x^2}} \frac{dy}{\sqrt{1-y^2}} \text{Re} \left\{ \frac{-\alpha + i[x - y]}{(1 + (-\alpha + i[x - y])^2)^{3/2}} \right\}, \quad (\text{A.5})$$

and consider only contribution of two small regions  $\{1 - x \ll 1, y \ll 1\}$  and  $\{x \ll 1, 1 - y \ll 1\}$ . After a lengthy but rather simple algebra we obtain

$$I_2^{(2)} = \frac{1}{\pi}$$

arriving at answer (54).

## References

- [1] Mirlin A D, Fyodorov Y V, Dittes F M, Quezada J and Seligman T H 1996 *Phys. Rev. E* **54** 3221
- [2] Evers F and Mirlin A D 2000 *Phys. Rev. Lett.* **84** 3690  
Evers F and Mirlin A D 2000 *Phys. Rev. B* **62** 7920
- [3] Kravtsov V E and Muttalib K A 1997 *Phys. Rev. Lett.* **79** 1913
- [4] Hu B B, Li B W, Liu J and Gu Y 1999 *Phys. Rev. Lett.* **82** 4224
- [5] Altshuler B L and Levitov L S 1997 *Phys. Rep.* **288** 487
- [6] Levitov L S 1990 *Phys. Rev. Lett.* **64** 547  
Levitov L S 1999 *Ann. Phys., Lpz.* **8** 697

- [7] Kravtsov V E and Tselik A M 2000 *Phys. Rev. B* **62** 9888
- [8] Calogero F 1969 *J. Math. Phys.* **10** 2191  
Calogero F 1969 *J. Math. Phys.* **10** 2197  
Calogero F 1971 *J. Math. Phys.* **12** 419  
Sutherland B 1971 *J. Math. Phys.* **12** 246  
Sutherland B 1971 *J. Math. Phys.* **12** 251
- [9] García-García A M and Verbaarschot J J M 2003 *Phys. Rev. E* **67** 046104
- [10] Moshe M, Neuberger H and Shapiro B 1994 *Phys. Rev. Lett.* **73** 1497
- [11] Gaudin M 1966 *Nucl. Phys.* **85** 545
- [12] Chalker J T, Kravtsov V E and Lerner I V 1996 *JETP Lett.* **64** 386  
Kravtsov V E 1999 *Ann. Phys. Lpz.* **8** 621
- [13] Ndwana M L and Kravtsov V E 2003 *J. Phys. A: Math. Gen.* **36** 3639
- [14] Abramowitz M and Stegun I A 1964 *Handbook of Mathematical Functions with Formulas, Graphs, and Mathematical Tables* (Washington, DC: National Bureau of Standards)
- [15] Efetov K 1997 *Supersymmetry in Disorder and Chaos* (Cambridge: Cambridge University Press)
- [16] Yevtushenko O and Kravtsov V E 2003 *J. Phys. A: Math. Gen.* **36** 8265
- [17] Yevtushenko O and Kravtsov V E 2004 *Phys. Rev. E* **69** 026104
- [18] Gradshteyn I S, Ryzhik I M, Jeffrey A and Zwillinger D 2000 *Table of Integrals, Series, and Products* (San Diego, CA: Academic)
- [19] Ossipov A and Kravtsov V E 2006 T-duality in supersymmetric theory of disordered quantum systems *Phys. Rev. B* **73** 033105